(2) Flory, P. J. *Statistical Mechanics of Chain Molecules*; Interscience: New York, 1969.
(3) Williams, A. D.; Flory, P. J. *J. Polymer Sci., A-2* **1967**, *5*, 417.
(4) Riande, E. *J. Polym. Sci., Polym. Phys. Ed.* **1977**, *15*, 1397.
(5) Riande, E.; Guzman, J.; Tarazona, M. P.; Saiz, E. *J. Polym. Sci., Polym. Phys. Ed.* **1984**, *22*, 917.
(6) Riande, E.; Guzman, J.; Llorente, M. A. *Macromolecules* **1982**, *15*, 298.
(7) Mendicuti, F.; Saiz, E. *Polym. Bull.* **1984**, *11*, 533; *Makromol. Chem.* **1986**, *187*, 2483.
(8) Riande, E.; Guzman, J. *J. Polym. Sci., Polym. Phys. Ed.* **1985**, *23*, 1235.
(9) Riande, E.; Guzman, J.; de Abajo, J. *Makromol. Chem.* **1984**, *185*, 1943.
(10) Riande, E.; de la Campa, J. G.; Schlereth, D. D.; de Abajo, J.; Guzman, J. *Macromolecules* **1987**, *20*, 1641.
(11) Mendicuti, F.; Viswanadhan, V. N.; Mattice, W. L. *Polymer* **1988**, *29*, 875.
(12) Mendicuti, F.; Patel, B.; Viswanadhan, V. N.; Mattice, W. L. *Polymer* **1988**, *29*, 1669.
(13) Bahar, I.; Mattice, W. L. *J. Chem. Phys.* **1989**, *90*, 6783.
(14) Actually, Flory, and many other authors after him, represent these two factors by σ_χ and σ_η. We have tried to simplify the nomenclature (see below) and used σ, σ_1, and σ_2 for the three first-order parameters in the analysis of these molecules.
(15) Abe, A.; Mark, J. E. *J. Am. Chem. Soc.* **1976**, *98*, 6468.
(16) Miyasaka, T.; Kinai, Y.; Imamura, Y. *Makromol. Chem.* **1981**, *182*, 3533.
(17) Miyasaka, T.; Yoshida, T.; Imamura, Y. *Makromol. Chem.* **1983**, *184*, 1285.
(18) San Roman, J.; Guzman, J.; Riande, E.; Santoro, J.; Rico, M. *Macromolecules* **1982**, *15*, 609.
(19) Bahar and Mattice (ref 13) obtain the energies of given conformations for pairs of bonds without separating the contributions E_σ, E_{σ_1}, etc. Consequently, these authors do not assign values to these parameters.
(20) Guggenheim, E. A. *Trans. Faraday Soc.* **1949**, *45*, 714; **1951**, *47*, 573.
(21) Smith, J. W. *Trans. Faraday Soc.* **1950**, *46*, 394.
(22) Mendicuti, F. *Rev. Sci. Instrum.* **1988**, *59* (5), 728.
(23) Saiz, E.; Suter, U. W.; Flory, P. J. *J. Chem. Soc., Faraday Trans. 2* **1977**, *73*, 1538.
(24) Flory, P. J. *Macromolecules* **1974**, *7*, 381.
(25) Suter, U. W.; Flory, P. J. *J. Chem. Soc., Faraday Trans. 2* **1977**, *73*, 1521.
(26) Irvine, P. A.; Erman, B.; Flory, P. J. *J. Phys. Chem.* **1983**, *87*, 2929.
(27) Abe, A.; Jernigan, R. L.; Flory, P. J. *J. Am. Chem. Soc.* **1966**, *88*, 631.
(28) Saiz, E.; Hummel, J. P.; Flory, P. J.; Plavsic, M. *J. Phys. Chem.* **1981**, *85*, 3211.
(29) Flory, P. J.; Saiz, E.; Erman, B.; Irvine, J. P.; Hummel, J. P. *J. Phys. Chem.* **1981**, *85*, 3215.
(30) Patterson, G. D.; Flory, P. J. *J. Chem. Soc., Faraday Trans. 2* **1972**, *68*, 1098.

Radical Trapping and Termination in Free-Radical Polymerization of MMA

S. Zhu, Y. Tian, and A. E. Hamielec*

Institute for Polymer Production Technology, Department of Chemical Engineering, McMaster University, Hamilton, Ontario, Canada L8S 4L7

D. R. Eaton

Department of Chemistry, McMaster University, Hamilton, Ontario, Canada L8S 4L7.
Received April 10, 1989; Revised Manuscript Received August 10, 1989

ABSTRACT: Post-effect measurements of radical concentrations for bulk free-radical polymerization of methyl methacrylate (MMA) at 25 °C with 5.0 wt % 2,2′-azobis(2-methylpropionitrile) (AIBN) initiated by an ultraviolet light (UV) were made by using an on-line ESR spectrometer. Number-average termination rate constants were therefrom directly measured by using radical decay rates. It was found that these termination rate constants decrease dramatically in the post-effect period at high conversions. These observations are in disagreement with the concept of termination by propagation–diffusion that was expected to be the dominant mode of termination at these high conversion levels. It was also found that a fraction of the radicals are trapped during the course of polymerization. In other words, there exist two radical populations in the reacting mass: free radicals and trapped radicals. The former is in the liquid state (as indicated by 13-line ESR spectra) while the latter are in solid state (9-line spectra). These two radical populations have very different reactivities in both propagation and termination reactions. Our data show that there is no minimum value of the termination rate constant for the long-lived trapped radicals. The trapped radical fractions measured directly herein suggest that heterogeneity in the polymerization medium can have a significant effect and must be properly accounted for when an analysis of the kinetics of polymerization is made.

Introduction

Although the termination reaction has been a matter of study for over 3 decades,[1] the molecular processes involved are not well understood, particularly at high conversions. The reasons for this lack of understanding are 2-fold. Firstly, the process itself is very complex, generally consisting of three definable steps. These include the following: two radical molecules migrate together via translational diffusion; the radical centers reorient by segmental diffusion; they overcome the chemical activation barrier and react. The activation energy for free radical reactions is quite small. The termination reaction is, therefore, likely to be diffusion-controlled, either segmental diffusion-controlled (usually at low polymer concentrations) or translational diffusion-controlled (at intermediate and high polymer concentrations). As polymer concentration increases, the macromolecular chains become

0024-9297/90/2223-1144$02.50/0

overlapped and entangled. This causes a significant reduction in termination rate, often referred to as the Trommosdorff or "gel" effect.[2] When macromolecules are significantly entangled so that the center-of-mass diffusion is essentially constrained, some theories[3,4] propose that the so-called termination by propagation–diffusion becomes the dominant mode of termination. Eventually when the reacting mass approaches its glassy-state transition and diffusion coefficients of small molecules such as monomers and primary radicals also fall appreciably, not only termination rate but also propagation and initiation rates fall dramatically.

On the other hand, experimental verification of the above termination mechanisms requires accurate experimental data whose interpretation is not model-dependent. There exists poor agreement among experimental data in the literature. To some extent, this is due to the fact that some conventional experimental techniques employ questionable assumptions. One among the many others is the use of measured reaction rates to monitor radical concentration changes. This assumes that all radicals behave identically in terms of propagation and termination. These methods are likely not applicable at high conversions where radicals may have different conformations, environments, and therefore reactivities.[5,6]

The advent of modern ESR techniques has provided a powerful direct method of radical type and concentration measurement. However, two difficulties are often met in its applications to free-radical polymerization. The first is the need to improve sensitivity to accurately measure low radical concentrations (about 10^{-7} mol/L), which are commonly found at low monomer conversions, and to provide a method that is able to detect rapid changes of radical concentration during pre- and post-effect periods. To some extent, this has been solved by Kamachi et al.[7] and Bresler et al.[8] The second is to give a precise interpretation of the details of the ESR spectra. In a previous paper,[6] we represented a model simulation of ESR spectra for MMA polymerization.

In this paper, we report on the use of an on-line ESR to measure radical concentration during post-effect periods at different conversions and to evaluate termination rate constants directly. The main interest is in the post-effect investigation of radical concentration as it provides great insight into polymerization mechanisms and kinetics.[23] Another incentive is the lack of understanding of concepts such as termination by propagation–diffusion, radical trapping, heterogeneity of reacting mass, and others.

Experimental Section

MMA (Fisher Scientific) was purified as follows: washed with a 10 wt % aqueous KOH solution to remove inhibitor, washed with deionized water, dried successively with anhydrous sodium sulfate and 4-Å molecular sieves, and then distilled under reduced pressure to provide a useful middle fraction. AIBN (Eastman Kodak) was recrystallized three times from absolute methanol.

A Pyrex ampule of 3-mm o.d. filled with reactants was inserted into a TM110 cavity of a Bruker ER100D ESR spectrometer. Polymerization was implemented on-line to avoid changes in radical type and concentration during quenching. The reaction temperature was controlled by a gas bath at 25 ± 0.5 °C. AIBN (5.0 wt %) was used for the polymerization.

It is clear that such a high initiator concentration may have some solvent effect on polymerization. The reason for the use of such a high initiator concentration was to achieve ESR signals with high signal to noise ratio for good quantitative analyses, particularly at low conversions where radical concentrations are usually very low.

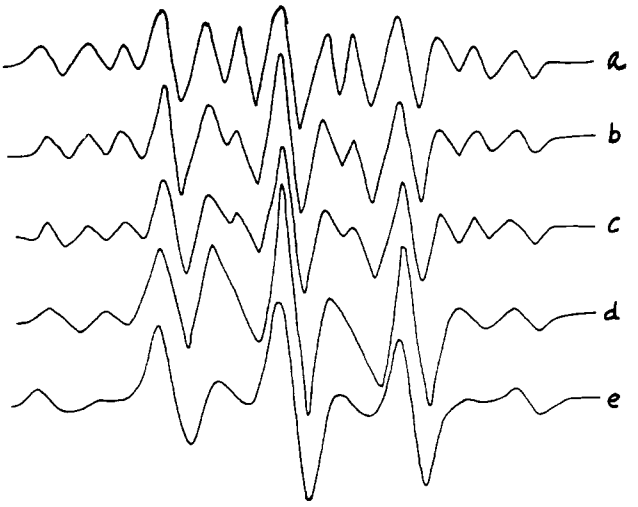

Figure 1. ESR spectra at various polymerizing times for the bulk polymerization of MMA at 25 °C with 5.0 wt % AIBN initiated by UV light. Operation conditions: microwave frequency, 9.45 GHz; modulation frequency, 100 KHz; modulation amplitude, 3.2 Gpp. Gain: (a–d) 1×10^6; (e) 5×10^4. Polymerizing times (min): (a) 2; (b) 32; (c) 45; (d) 52; (e) 120.

Polymerization was initiated with a UV light. Radical spectra were recorded frequently to follow the polymerization in detail. To measure post-effect changes in radical concentration, we monitored the decays of radical concentration after illumination had been stopped to cease generation of AIBN radicals. At low conversions, ESR signal decay rates are so rapid that there is insufficient time to scan a whole ESR spectrum (e.g. 90% of the radicals disappear in <1 s, with $[R^\bullet]_0 = 10^{-6}$ mol/L, $K_t = 10^7$ L/(mol s)), the ESR pen was fixed to a central line peak, and a chart recorder was used to record the decays in ESR spectra (see Figure 8).

Absolute radical concentrations were calibrated by using 2,2-diphenyl-1-picrylhydrazyl hydrate (DPPH) (Aldrich Chemicals) dissolved in MMA using the same type of ampule. Peak broadening of MMA radical spectra were also corrected by using $[R^\bullet] \propto HL_{pp}^2$[9] where H and L_{pp} are height and width of central line, respectively.

Monomer conversions were measured by using a Raman spectrometer[10] (conventional Spex, cat. 14018, ser. 5420, double-monochromator, 0.85 m, 1800 grooves/mm).

Results and Discussion

Figure 1 shows some ESR spectra obtained during the course of polymerization. (The spectra recorded at the early stage of polymerization were smoothed prior to being incorporated into the present figures.) The first one (a) is typical 13-line spectrum that is attributed to MMA radicals in liquid state, while the last (e) is a 9-line spectrum attributed to radicals in the solid state. The ESR spectrum experiences a transition from 13-line to 9-line spectrum during polymerization. Our model simulations[6] reveal that the intermediate spectra (b–d) are due to an overlap of 13-line and 9-line spectra having different intensities. This strongly suggests that there exist two populations of radicals, radicals in the liquid and solid states, in the reacting mass. In other words, the reacting mass is heterogeneous in terms of radical environment. This will be discussed more fully later.

Figure 2 shows the radical concentration history during the polymerization. The radical concentration is relatively constant at low concentrations, i.e., $d[R^\bullet]/dt \approx 0$, but then there is a dramatic increase in concentrations and finally a leveling off. The dramatic rise in radical concentration corresponds to the usually observed autoacceleration in polymerization rate. This phenomenon is often referred to as the Trommosdorff effect or

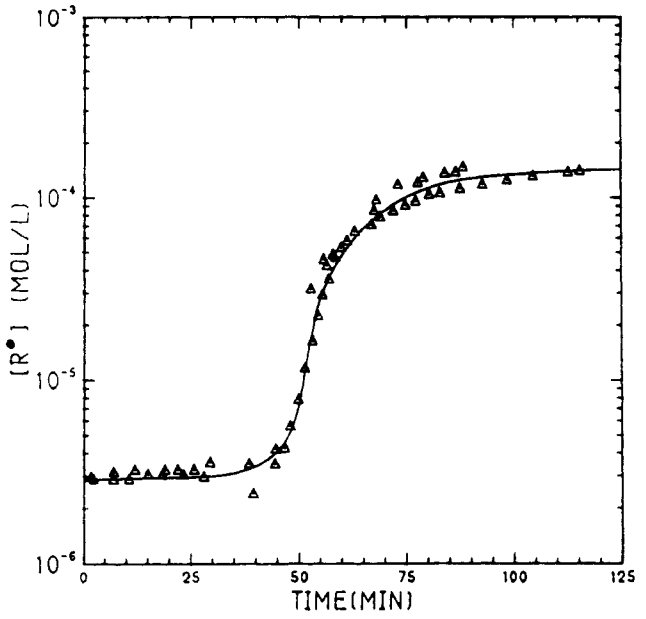

Figure 2. Total radical concentration ([R•], mol/L) versus polymerizing time (t, min) for bulk polymerization of MMA at 25 °C with 5.0 wt % AIBN initiated by UV light.

"gel" effect.[2] The transition of the ESR spectrum from 13-line to 9-line is complete during this autoacceleration.

Parts A and B of Figure 3 show the changes in radical concentration during the post-effect period at different levels of conversion. It can be seen that the radical concentration rapidly decays at low conversions, as expected, taking only a few seconds. This confirms that the risk of loss of radicals using those methods that quench the reaction before ESR measurement is real. On-line measurement by ESR is preferred. Termination rate constants can be directly evaluated from these post-effect measurements by using eq 1,

$$d[R^\bullet]/dt = -\bar{K}_{tn}[R^\bullet]^2 \quad (1)$$

where $\bar{K}_{tn}$ is the number-average termination rate constant,[21] defined as $\sum_1^\infty\sum_1^\infty K_t(i,j)\Phi^\bullet(i)\Phi^\bullet(j)$, $K_t(i,j)$ is an arbitrary chain length dependent termination rate constant for radicals with chain lengths i and j, and $\Phi^\bullet(i)$ and $\Phi^\bullet(j)$ are corresponding number fractions of these radicals. Equation 1 may be rearranged into a more convenient form as follows:

$$\bar{K}_{tn} = d(1/[R^\bullet])/dt \quad (2)$$

Parts A and B of Figure 4 plot the reciprocal of radical concentration ($1/[R^\bullet]$) as a function of time (t). Evaluation of the initial slopes for these curves gives the termination rate constants ($\bar{K}_{tn}$) shown in Figure 5.

Termination rate constant variation with conversion can be divided into four regimes. Initially ($X < 0.15$), $\bar{K}_{tn}$ is relatively constant. In this regime, the termination rate is segmental diffusion-controlled. $\bar{K}_{tn}$ thus measured is not a chemical reaction rate constant, segmental reorientation rate is actually involved, and therefore $\bar{K}_{tn}$ is a function not only of temperature but also of radical molecular properties, such as size, chain rigidity, etc. At some conversion ($X \approx 0.15$), $\bar{K}_{tn}$ starts to fall dramatically. The generally accepted explanation for this is that macromolecular chains become overlapped and then entangled. This entanglement reduces macromolecular center-of-mass diffusion rates appreciably for translational diffusion to be rate-determining. Recently, many models

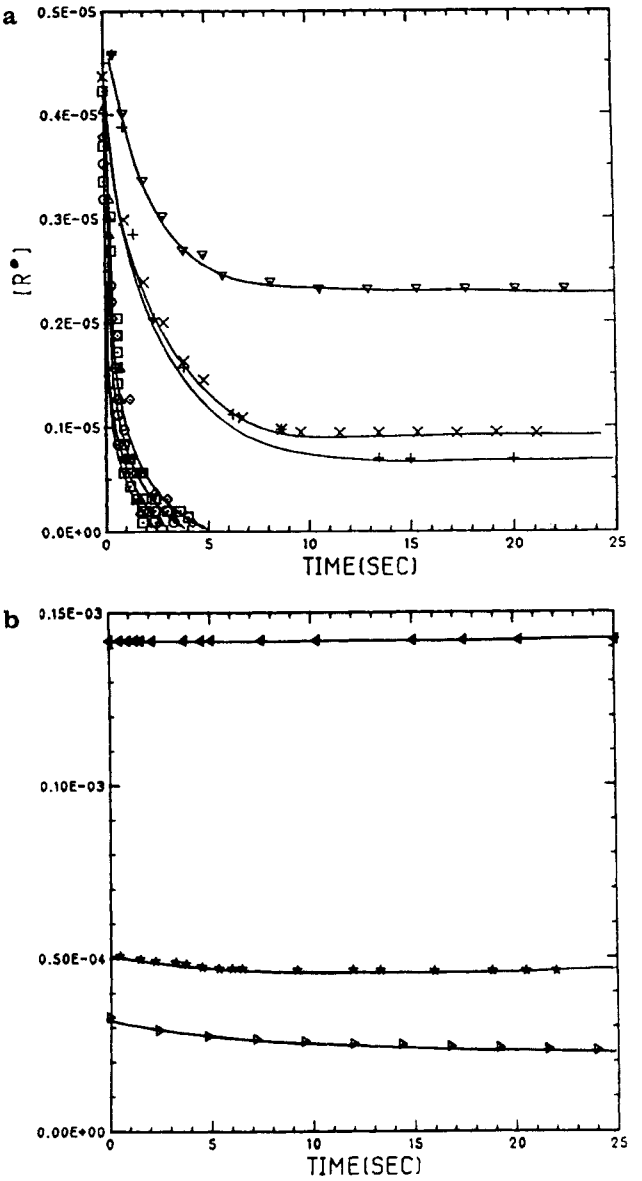

Figure 3. Total radical concentration ([R•], mol/L) decay during post-effect period for bulk polymerization of MMA at 25 °C. Conversion levels: A, (⊙) 0.00, (▲) 0.05, (⊡) 0.10, (◇) 0.13, (+) 0.22, (×) 0.23, (▽) 0.31; B, (◁) 0.37, (☆) 0.65, (▷) 0.78.

(see ref 11–15 for a review of these models) have been proposed to give quantitative descriptions for this reduction. Many of these models are based on totally different theories, such as free volume concepts, reptation scaling law, etc., but appear equally effective in describing conversion histories and molecular weight developments. Obviously, this situation is due to lack of crucial experimental data.

After an order-of-magnitude decrease ($X \approx 0.35$), the termination rate constant levels off and shows a plateau up to a conversion of about 0.70. Finally ($X > 0.70$), $\bar{K}_{tn}$ experiences a second dramatic fall. This fall is attributed to the glassy effect, where diffusion rates of small molecules such as monomers and primary radicals fall significantly. It has been proposed[3,4] that at these late stages of polymerization, a polymer radical loses its center-of-mass mobility and propagation–diffusion becomes the dominant mode of termination.

By propagation–diffusion means that an active chain end diffuses via propagation. In other words, a propagation step contributes to the migration of a radical center. Russell et al.[3] have derived an equation for the dif-

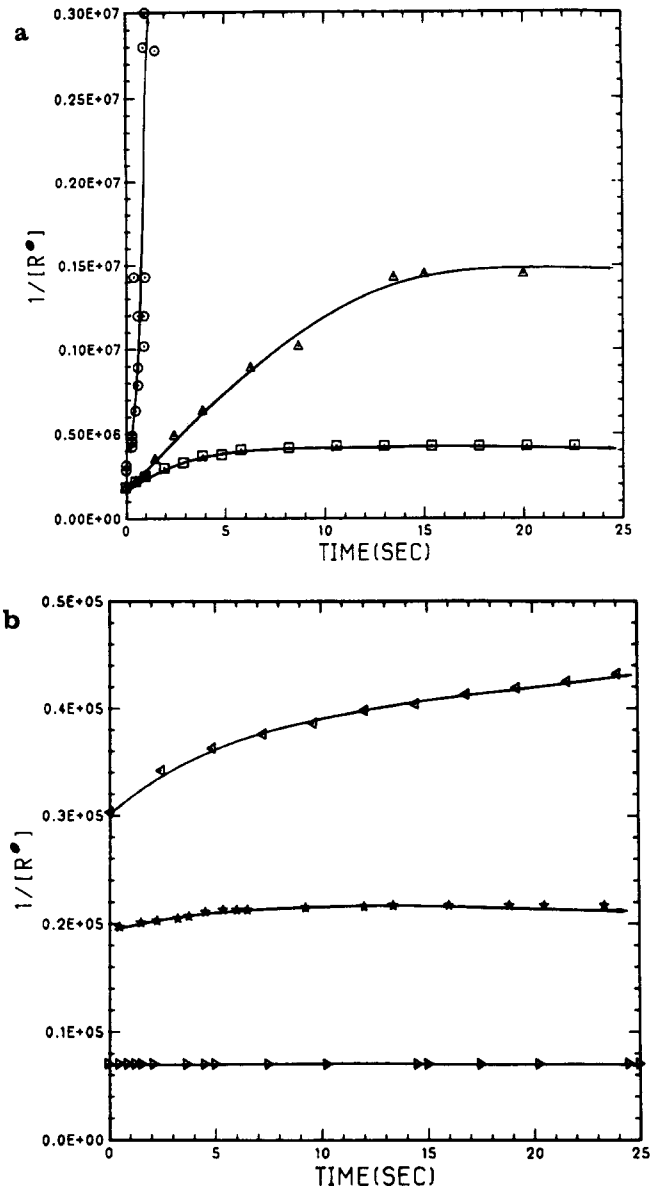

Figure 4. Reciprocal of radical concentration (1/[R•], L/mol) versus polymerizing time (t, s) during post-effect period for bulk polymerization of MMA at 25 °C. Conversion levels: A, (⊙) 0.00, (▲) 0.23, (⊡) 0.31; B, (◁) 0.37, (☆) 0.65, (▷) 0.78.

fusion coefficient (D) of the radical center (eq 3), where

$$D = K_p[M]a^2/6 \tag{3}$$

K_p is the propagation rate constant, [M] is monomer concentration, and a is the root-mean-square end-to-end distance per square root of the number of monomer units in the polymer chain (0.69 nm for PMMA). Such diffusion behavior (D) is a prerequisite for modeling the termination rate constant (K_t). Relationships of K_t as a function of the diffusion coefficient (D) for macroradicals is not well developed. A most often used model is[16]

$$K_t = 4\pi r' D' \tag{4}$$

where D' is the mutual diffusion coefficient (= $2D$) and r' is the distance within which two radicals overcome the chemical activation barrier and terminate. This distance is often taken as the sum of radii of the two reactants (= $2r$). Substitution of eq 3 into eq 4 yields

$$K_t = 8\pi K_p[M]a^2 r/3 \tag{5}$$

for termination by propagation diffusion. An estimation of K_t using r' = 5.85 Å (Lennard-Jones diameter of MMA[16]) usually gives a value that is an order of magnitude lower than that found by experiment. Therefore, some effort has been made recently to develop models for the reaction radius (r) to explain this discrepancy. These models focus on macroradical chain entanglement and often take the node of entanglement with the dangling chain as a diffusing sphere. A straightforward result by Russell et al.[3] is $j_c^{1/2}a$ for a flexible polymer chain where j_c is an average number of monomeric units between two successive nodes or equally in a dangling chain. Another more complex approach by Soh and Sundberg[4] is $(1/p)\{\ln [p^3/(\pi^{3/2}N_{av}[R^\bullet])]\}^{1/2}$ where $p^2 = 3/(2j_ca^2)$. This is derived by equating bulk radical concentration to a local radical concentration that has a Gaussian distribution about the entanglement node (Soh and Sundberg also use the "volume-swept-out" model instead of the Smoluchowski equation and $D/j_c^{1/2}$ for the node diffusion coefficient).

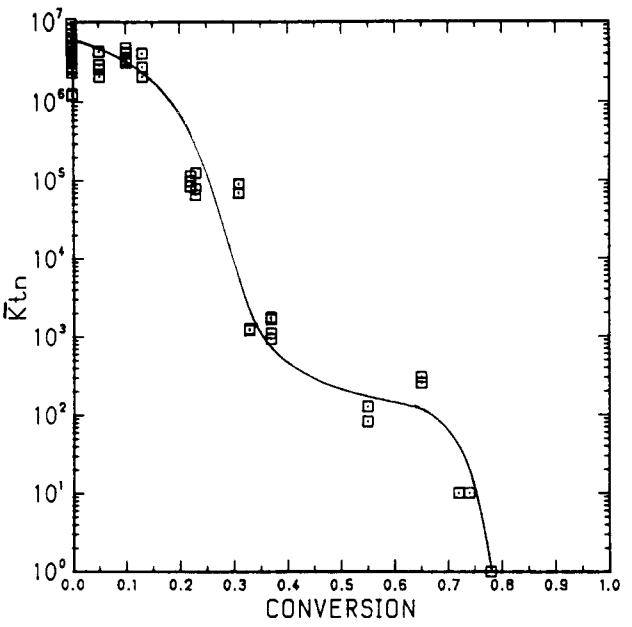

Figure 5. Number-average termination rate constant ($\bar{K}_{tn}$, L/(mol s)) versus conversion (X) for bulk polymerization of MMA at 25 °C with 5.0 wt % AIBN initiated by UV light.

Although the above models give reasonable predictions for the behavior of the number-average termination rate constant versus conversion at the late stages of polymerization (Figure 5), they have not been tested under reaction conditions, such as termination in the post-effect period. As it has already been seen in Figure 4, the curves of 1/[R•] versus t are not straight lines for high conversions. In other words, $\bar{K}_{tn}$ is not constant during the post-effect periods. We have estimated these $\bar{K}_{tn}$ values by using eq 2 and plot three of them in Figure 6. The corresponding model predictions are also plotted in the same figure. A point worth mentioning here is that there are two macromolecule populations in the reacting mass of a free-radical polymerization, polymer radicals and polymer molecules. Except for times near zero, the weight of radicals is negligible and therefore the possible change in conversion or [M] during post-effect periods is also negligible. Given the K_p values (43.6 L/(mol s) at X = 0.37; 39.5 L/(mol s) at X = 0.65, this work via ESR plus rate measurements) and the reaction distance r' ((1) Lennard-Jones diameter for minimum, (2) entanglement spacing $j_c^{1/2}a$ (j_c = 100 for MMA[17]) for maximum, and (3) Soh and Sundberg's approach), eq 5 gives the termination rate constant as straight lines for the first two cases

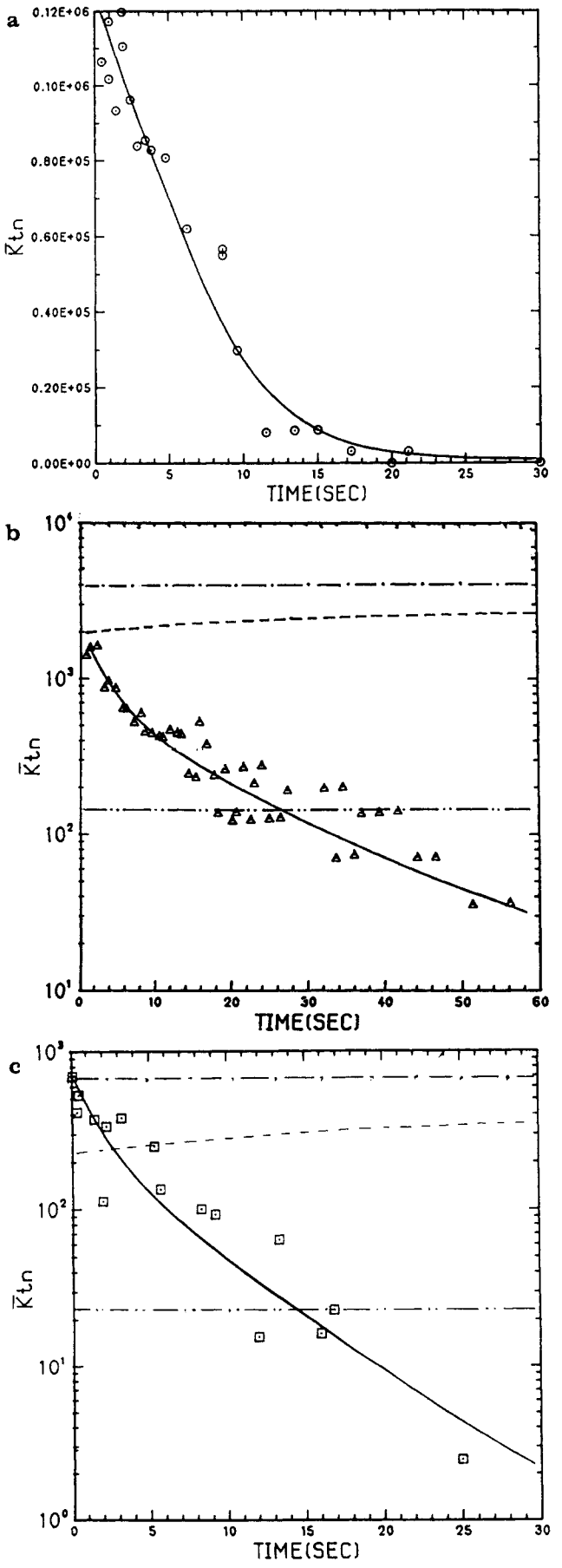

Figure 6. Number-average termination rate constant ($\bar{K}_{tn}$, L/(mol s)) behavior during post-effect period for bulk polymerization of MMA at 25 °C. Conversions levels: A, (⊙) 0.23, B, (▲) 0.37; C, (⊡) 0.65; (- - -) Soh and Sundberg's prediction;[4] minimum (– ·· –) and maximum (– · –), eq 5, Russel et al.[3]

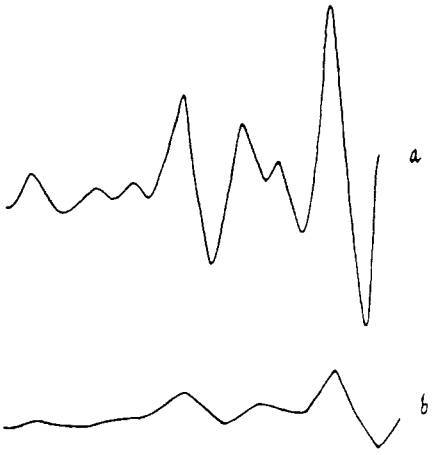

Figure 7. Structural change of an ESR spectrum during post-effect period: gain, 10^6; UV illumination, 47 min; (a) Before turning off UV light; (b) 60 s after radical generation ceases.

and with a slight increase due to the decrease in radical concentration for the last case. The discrepancies between the model predictions and our experimental data are clearly seen in Figure 6. It can be concluded that (1) the apparent termination rate constants decrease significantly rather than remain constant during the post-effect periods even at high conversions and (2) there exist no minimum limits in these rate constants that actually approach zero in late post-effect times.

We have also examined the possible radical concentration dependence of termination rate constant according to Chiu, Carratt, and Soong[18]

$$1/\bar{K}_{tn} = 1/K_{t0} + r^2[R^\bullet]/3D \qquad (6)$$

where K_{t0} is a chemically controlled termination rate constant. Equation 6 is equivalent to eq 3 under the conditions of $(4/3)\pi r^3[R^\bullet] = 1$ and $K_{t0} \gg 4\pi r'D'$. Obviously such a radical concentration dependence given by eq 6 is also in conflict with our experimental observations. A careful examination of the derivation of eq 6 reveals that the radical concentration dependence is not necessary because the axis is set on one radical center; i.e., $(4/3)\pi r^3[R^\bullet] = 1$.

In general, the number-average termination rate constant is a function of the sizes of terminating radicals, molecular weight distribution and concentration of accumulated polymer, and temperature. The decrease in $\bar{K}_{tn}$ during the post-effect period may be attributed to the more rapid consumption of low molecular weight radicals with chain lengths less than j_c. Although the weight fraction of such small radicals may be small, the role they play in termination can be important because of their possible large number fraction and their larger diffusion rates due to reptation[19] ($D_1 j^{-\alpha}$, where D_1 is the diffusion coefficient of the primary radical and $\alpha = 2$) rather than via propagation. A rough estimation (given $D_1 = 10^{-7}$ cm^2/s[20]) shows that radicals with chain lengths less than 10^3 (monomeric units) have higher diffusion coefficients than the propagation–diffusion coefficient, D_{p-d} ($\approx 10^{-13}$) cm^2/s, eq 3).

Another major reason for the complex behavior of the termination rate constant during the post-effect period is a radical trapping effect. There is clear evidence, from the structural change in the ESR spectra, that some radicals are trapped during the course of polymerization. Consider the following experiment: Expose the contents of an ampule to UV illumination and record the ESR spectra frequently up to a conversion where the autoacceler-

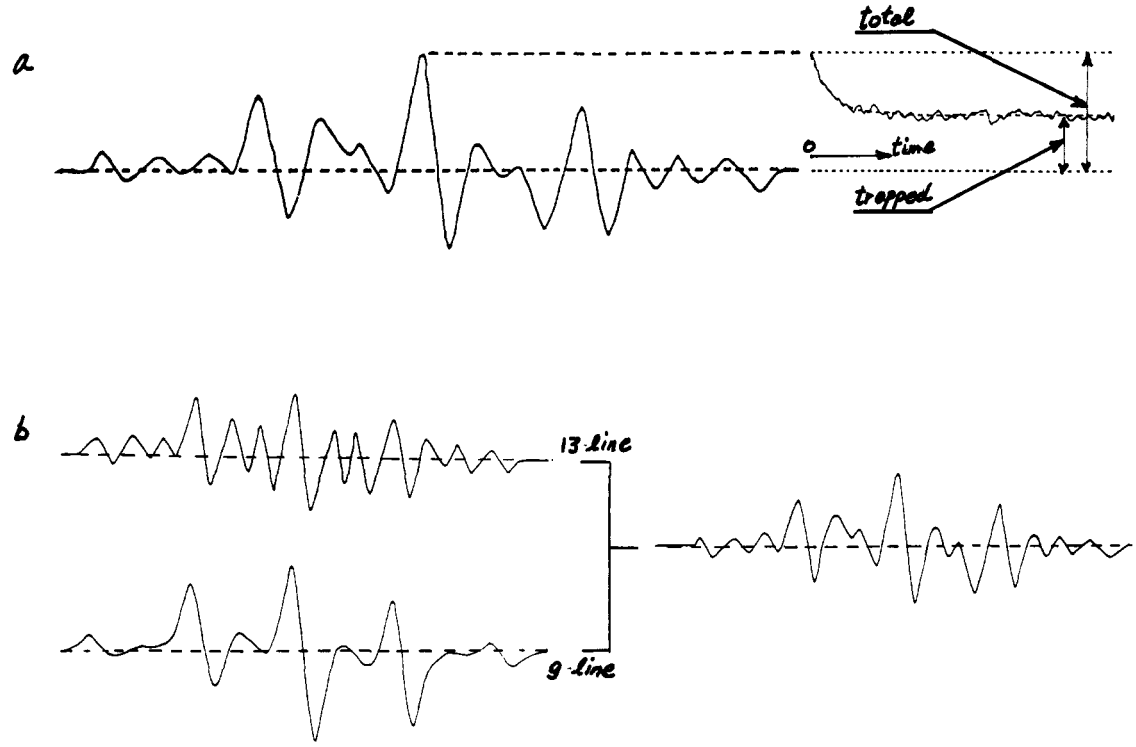

Figure 8. Illustration for measurement of trapped radical fraction ($[R^\bullet]_{trapped}/[R^\bullet]_{total}$): (a) monitor height decay in central line of ESR spectrum after turning off UV light; (b) extract 9-line component from ESR spectrum (see ref 6).

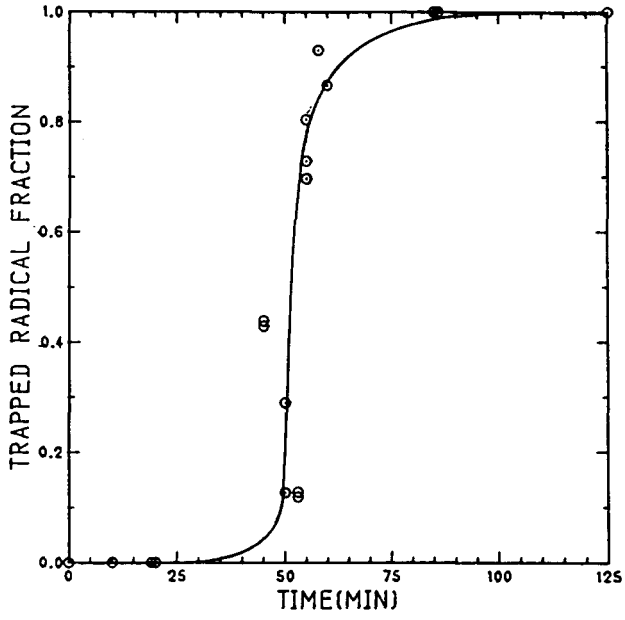

Figure 9. Trapped radical fraction ($[R^\bullet]_{trapped}/[R^\bullet]_{total}$) versus reacting time ($t$, min) for bulk polymerization of MMA at 25 °C with 5.0 wt % AIBN initiated by UV light.

ation in rate appears but the ESR signal still has 13 lines as shown in Figure 7a, which is in fact an overlap of a standard 13-line spectrum from MMA radicals in the liquid state and a 9-line spectrum from MMA radicals in the solid state. Then turn off the UV light source to stop the generation of radicals. The ESR signal decays significantly. Scan another ESR spectrum after some minutes. The signal is found to be a 9-line spectrum as shown in Figure 7b. The 13-line component disappears from the overlapped spectrum. In other words, those mobile free radicals that provide the 13-line signal are consumed by termination. The residue radicals that give the 9-line signal are quite stable demonstrating a very low reactivity (survive for months[6]).

The amount of trapped radicals can be estimated either (1) by measuring the residue signals during the post-effect period or (2) by extracting the 9-line component from an overlapped spectrum. The former method requires post-effect ESR measurement. As illustrated in Figure 8a, the final height of central line over the initial value (height at $t = 0$) gives a number fraction of trapped radicals ($[R^\bullet]_{trapped}/[R^\bullet]_{total}$). On the other hand, as shown in Figure 8b, the latter method requires ESR spectrum deconvolution. It is known that the ESR spectra recorded during the course of polymerization are actually mixed spectra that are composed of both 13-line and 9-line spectra. These two spectra can be estimated. An evaluation of the relative strength of the 9-line spectrum gives the fraction of trapped radicals (see ref 6 for details). Figure 9 presents such measured data (obtained by the method of Figure 8a). It can be seen that the value of the trapped radical fraction increases dramatically from 0 to 1 during the rapid growth in radical concentration. This suggests that a strong relationship exists between the autoacceleration and radical trapping.

The coexistence of mobile radicals and trapped radicals suggests that the reacting mass is heterogeneous in terms of radical environment. The physical picture of this is as follows. During the autoacceleration, macroradicals (radicals with long chains) are entangled by environmental polymer matrix, and therefore the terminations for these radicals are seriously constrained. But propagation may still be chemically controlled. As a result, these macroradical chains become even longer and monomer concentrations in the vicinity of radical centers are exhausted; therefore these radical centers experience a solid environment that consists of polymer chains. However, small radicals are still free to both propagate and terminate. Obviously, such heterogeneity of the reacting mass seriously confounds the polymerization mechanisms and makes it very difficult to do kinetic analyses. One among many others is that the propagation rate constant must be well-defined. The two radical popula-

tions have different reactivities not only in termination but also in propagation because the trapped radicals in fact are not readily accessible to monomers. The probability of a radical center becoming trapped is a strong function of its chain length, and therefore, chain length dependent propagation as well as termination may be relevant. Any attempt at modeling such a polymerization process must properly account for these radical trapping effects.

Acknowledgment. Financial assistance from the Natural Sciences and Engineering Research Council of Canada, the Ontario Center for Materials Research, and the McMaster Institute for Polymer Production Technology are appreciated.

References and Notes

(1) Benson, S. W.; North, A. M. *J. Am. Chem. soc.* **1959**, *81*, 1339.
(2) Trommsdorff, E.; Kohle, H.; Lagally, P. *Makromol. Chem.* **1948**, *1*, 169.
(3) Russell, G. T.; Napper, D. H.; Gilbert, R. G. *Macromolecules* **1988**, *21*, 2133.
(4) Soh, S. K.; Sundberg, D. C. *J. Polym. Sci., Polym. Chem. Ed.* **1982**, *20*, 1315.
(5) Zhu, S.; Tian, Y.; Hamielec, A. E.; Eaton, D. R. Radical Concentrations in Free Radical Copolymerization of MMA/EGDMA. *Polymer*, in press.
(6) Tian, Y.; Zhu, S.; Hamielec, A. E.; Eaton, D. R., Conformation, Environment and Reactivity of Radicals in Copolymerization of MMA/EGDMA. *Polymer*, submitted for publication.
(7) Kamachi, M.; Kuwae, Y.; Kohno, M.; Nozakura, S. *Polym. J.* **1985**, *17*, 541.
(8) Bresler, S. E.; Kozbekov, E. N.; Fomichev, V. N.; Shadrin, V. N. *Makromol. Chem.* **1974**, *175*, 2875.
(9) Shen, J.; Tian, Y.; Zeng, Y.; Qiu, Z. *Makromol. Chem., Rapid Commun.* **1987**, *8*, 615.
(10) Chu, B.; Lee, D. *Macromolecules* **1984**, *17*, 926.
(11) Cardenas, J. N.; O'Driscoll, K. F. *J. Polym. Sci., Polym Chem. Ed.* **1976**, *16*, 348.
(12) Marten, F. L.; Hamielec, A. E. *ACS Symp. Ser.* **1978**, *No. 104*, 43.
(13) Ito, K. *J. Polym. Sci., Polym. Chem. Ed.* **1977**, *15*, 1759.
(14) Tulig, T. J.; Tirrell, M. *Macromolecules* **1981**, *14*, 1501.
(15) Soh, S. K.; Sundberg, D. C., *J. Polym. Sci., Polym. Chem. Ed.* **1982**, *20*, 1299.
(16) Smoluchowski, M. *Z. Phys. Chem.* **1917**, *92*, 129.
(17) Ferry, J. D. *Viscoelastic Properties of Polymers*; Wiley-Interscience: New York, 1970.
(18) Chiu, W. Y.; Carratt, G. M.; Soong, D. S. *Macromolecules* **1983**, *16*, 348.
(19) de Gennes, P. G. *Scaling Concepts in Polymer Physics*, Cornell University Press: Ithaca, NY, 1979.
(20) Hwang, D.; Cohen, C. *Macromolecules* **1984**, *17*, 2890.
(21) Zhu, S.; Hamielec, A. E. Chain Length Dependent Termination in Free Radical Polymerization. *Macromolecules* **1989**, *22*, 3093.
(22) Reid, R. C.; Sherwood, T. K. *Properties of Gases and Liquids: Their Estimation and Correlation*; McGraw-Hill: New York, 1958.
(23) Tian, Y. Ph.D. Thesis, Jilin University, China, 1988.

Registry No. MMA, 80-62-6.

Theoretical Investigation of Gas-Phase Torsion Potentials along Conjugated Polymer Backbones: Polyacetylene, Polydiacetylene, and Polythiophene

J. L. Brédas*,† and A. J. Heeger

Institute for Polymers and Organic Solids, University of California, Santa Barbara, California 93106. *Received April 27, 1989; Revised Manuscript Received July 22, 1989*

ABSTRACT: We present ab initio quantum-chemical calculations on the gas-phase torsion potentials of oligomers representative of polyacetylene, polydiacetylene, and polythiophene. Our goal is to obtain reliable values for the total energies involved in the torsions of fully conjugated chains, in order to assess the flexibility of such chains in solution and to provide the basis for meaningful discussions of persistence length and conjugation length models. Rotation around a single bond leads to barrier heights on the order of a few kilocalories per mole in polyacetylene and polythiophene (about 6 and 3 kcal/mol, respectively) but lower than 1 kcal/mol in polydiacetylene.

I. Introduction

One of the major advances in the field of conducting polymers has been the recent advent of conducting polymer solutions. Solutions of poly(*p*-phenylene sulfide) were first obtained by Frommer and co-workers; however, the solvents were rather exotic, such as an arsenic trifluoride–arsenic pentafluoride mixture.[1,2] More recently, Elsenbaumer et al.,[3] Sato et al.,[4] and Hotta et al.[5] turned their interest to polythiophene and found that the addition of long flexible alkyl chains (containing four or more carbons) on position 3 of the thiophene rings allows the polymer chains to become soluble in common organic solvents such as chloroform, dichloromethane, or tetrahydrofuran. The addition of an ethane- or butanesulfonate group, as considered by Wudl et al. or Meijer et al.,[6] renders the polymer chains soluble in water and leads to the concept of self-doped polymers when the chains are oxidized.

Intrinsic solubility (i.e., without side-chain addition) has been discovered for polyaniline. This polymer is soluble in concentrated sulfuric acid[7] and partially (or in some cases completely) soluble in organic solvents.[8]

These discoveries open the way to more complete characterization of conducting polymers as macromolecules

† Permanent address: Service de Chimie des Matériaux Nouveaux, Département des Matériaux et Procédés, Université de Mons, B-7000 Mons, Belgium.

0024-9297/90/2223-1150$02.50/0